05

Analysis of the soot particles structure in a flame by Raman spectroscopy

© E.V. Gurentsov[1], A.V. Eremin,[1] R.N. Kolotushkin,[1] E.S. Khodyko[1,2]

[1] Joint Institute for High Temperatures, Russian Academy of Sciences,
125412 Moscow, Russia
[2] N.E. Bauman Moscow State Technical University,
105005 Moscow, Russia
e-mail: kolotushkin.roman@gmail.com

Received May 5, 2023
Revised March 6, 2024
Accepted March 7, 2024

The influence of the fuel type on the structure of soot particles formed in laminar pre-mixed flames of ethylene–air and acetylene–air was analyzed. The comparison was carried out between young soot at an intermediate stage of growth, and mature soot. The 1st order Raman spectra of sampled particles were analyzed and compared with each other. As a result of Raman spectra interpretation, it was obtained that for both fuels, during the growth of soot particles, the size of graphene layers increases, as well as the content of hydrogen in the particles decreases. Acetylene soot shows a more graphitized structure than ethylene soot.

Keywords: soot particles, laminar premixed flames, Raman spectroscopy, graphene layers, internal structure.

DOI: 10.61011/TP.2024.05.58519.119-23

Introduction

Study of structure of soot particles formed during combustion and pyrolysis of hydrocarbons, has great importance for practical applications [1], as structure of particles determines their properties (optical, thermophysical, electrical, etc.). The proper accounting of optical properties is necessary to determine contribution of sun radiation absorption by soot particles to the thermal balance of atmosphere affecting the climate changes [2]. Monitoring of soot particles produced both during anthropogenic impact on the environment, as well as, for example, during natural fires, is based on optical measurements. Using these data we can evaluate the danger of soot emission for human health [3]. Besides, radiation and thermophysical properties of soot are important for calculations of thermal processes in combustion chambers of engines, boilers and other reactors. On other hand the carbon black is widely used as addition to create various products. It is used as reinforcing filler during tires production, as electric conduction connection in manufacturing of plastics, antistatic rubbers and anodic rubber grounding agents, and a black pigment for creating various types of paints and enamels. In each individual industry definite grades of carbon black are necessary, their selection can improve mechanical, electrical or painting properties of products.

Properties of soot particles are determined by their internal structure, which highly varies depending on conditions of their formation [4]. It is known, that one of the main factors determining structure of formed soot particles is exposure time in high temperature reactor, when transformation of the internal structure of soot particles occurs [4]. In our previous paper [5] we studied properties of soot particles in wide spectrum of their formation conditions. Hydrocarbon fuels were used with different tendency to soot formation (acetylene, ethylene, propylene, ethylene with dimethyl ether additives), and two fundamentally different reactors for particle synthesis (laminar flame and shock tube). It was shown that change in structure of soot particles (and, hence change in their properties) correlates well with their average size increasing. During growth of soot particles the spacing from 0.4–0.5 decreases between graphene layers, which composed the structure of the soot particles, from 0.4–0.5 nm to 0.35 nm, which is close to interplanar spacing in graphite (0.335 nm). Besides there is increase in zones of basic structural units (BSU), i.e. regions of dense stacked graphene planes similar to local regions of graphite. Both phenomena characterize graphitization of soot particles during their growth, i.e. transition from amorphous structure to partially ordered, reminiscent of graphite [6].

Values of optical and thermophysical properties, and parameters of internal structure depending on average size of particles obtained in papers [5,7] demonstrate the moderate scattering of their properties depending on type of fuel used for particles synthesis. This states that there is one more parameter affecting the process of formation and growth of soot particles. Method of transmission electron microscopy (TEM) does not ensure this parameter determination. It was decided to use another method of morphology analysis of condensed particles — Raman spectroscopy (RS). Changes in the sample structure are

presented as changes in profile of Raman spectrum and its parameters, such as intensity of peaks, their position and half-width.

It is known that this spectroscopic method is a common diagnostic for obtaining detailed information about the electronic and chemical structure of any carbon-based material [8] both for scientific studies and for production. For example, in production line of carbon black the portable Raman spectrometers are used, which ensure quick quality monitoring of final products without use of large-size and expensive laboratory units.

An overview published by A. Ferrari and co-authors presents the actual information on modern state of graphene analysis by method of Raman spectroscopy, as well as all its aspects [9]. When it comes to the soot particles studies, there is a number of recently published papers related to investigation of the particles synthesized in diesel and gasoline engines [10,11] and during detonation [12] via Raman spectroscopy method. In papers [13,14] the structure of soot particles obtained in premixed ethylene flame was analyzed by this method.

So, Raman spectroscopy is a common analytical method for studying the micro/nanostructure of soot [15]. The present paper objective is study of structure of soot particles by Raman method to determine effect of the fuel type on formed particles. It is necessary to study both soot particles that reached the limit of transformation of the internal structure (mature soot), and particles that are at an intermediate stage of growth (young soot). The present paper is a logical continuation of cycle of papers of authors [5,7,16]. Ethylene and acetylene were chosen as the fuels to be studied. Ethylene is recommended fuel to study the process of soot formation in laminar flames [17]. Selection of acetylene is determined by that it is one of the most important compound during soot formation regardless of type of initial fuel [18].

1. Research methods

1.1. Burner

As experimental reactor for soot nanoparticles synthesis a standard flat flame burner of McKenna type („Holthuis & Associates“) were used with porous surface of bronze 62 mm in diameter (Fig. 1). A brass disk 60 mm in diameter and 20 mm thick located height above burner (HAB) of 23 mm was used to stabilize the flame.

The burner has outer ring contour to supply shielding gas (N_2). This flow additionally stabilizes flame and isolates it from action of external disturbances. When the fuel/oxidizer ratio is above the stoichiometric one, a fraction of fuel is spent on heating the mixture during combustion, and soot particles form in the process of pyrolysis of the remaining fuel. In a one-dimensional structure of a flat flame, the molar fractions of substances and the temperature depend only on the height above burner. Compositions of

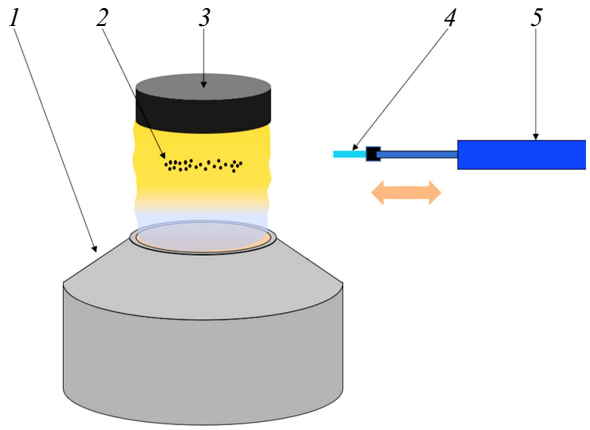

Figure 1. Experimental setup of soot particles sampling: *1* — McKenna burner, *2* — soot particles formed in flame, *3* — stabilizer, *4* — quarts plate, *5* — pneumatic cylinder.

Table 1. Compositions of mixtures in premixed flames used for soot structure analysis

Mixture	C_nH_m,%	O_2,%	N_2,%	[C]/[O]
Ethylene–Air	14.1	18	67.9	0.78
Acetylene–Air	13.3	18.4	68.3	0.72

fuel mixtures used for data analysis on the internal structure of soot particles are given in Table 1. The ethylene flame composition is the recommended mode for the study of soot formation in flame [17]. Composition of acetylene flame was selected such that the total gases flow rate and ratio [C]/[O] will be close to the ethylene mode, and at that the flame itself keeps stable, laminar and flat structure.

The flow rates of gases were monitored with RRG-10 („Eltochpribor“) mass flow controllers. For temperature monitoring along vertical and horizontal axes of flame the platinum-rhodium thermocouples type B with wire diameter 45μm and junction diameter 70μm was used. The actual gas temperature was estimated with convective and radiation heat losses in the flame and the deposition of soot particles on the thermocouple junction taken into account in accordance with the procedure outlined in [19]. Fig. 2 shows temperature profiles in center of studied flames, measured by microthermocouple method.

1.2. Sampling

McKenna burner forms one-dimensional flat flame. Height above the burner under the given conditions is analog of time of chemical reactions occurred during burning, including indicator of different stages of process of formation and growth of soot particles. Lower zones of flame (to height ~ 3 mm) correspond to stages of formation and growth of polyaromatic hydrocarbon (PAH) molecules,

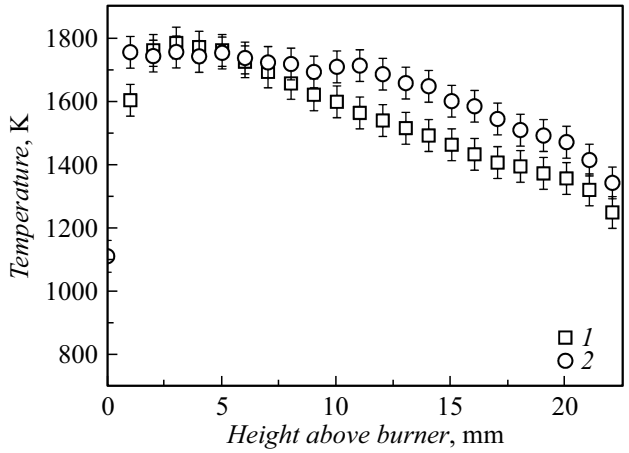

Figure 2. Temperature profiles in center of flame depending on HAB. Fuel mixture: *1* — ethylene–air, *2* — acetylene–air.

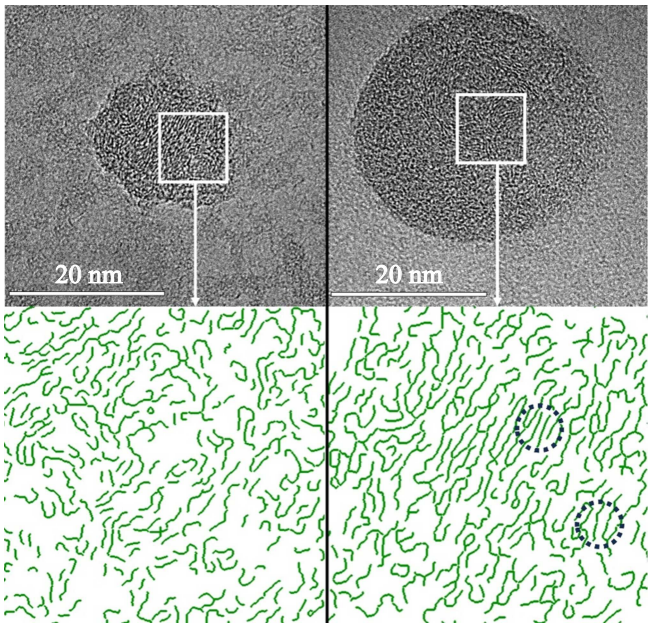

Figure 3. Examples of TEM image of soot particles (upper part) and location of graphene planes inside particles (bottom part) [5]. On left — young soot particle, on right — mature one. Highlighted areas — BSU zones.

which are precursors of soot particles. Middle zone of flame (height $\sim 3-8$ mm) corresponds to soot inception from PAH molecules and initial stage of growth of young soot particles. In top zones of flame (> 8 mm) this process actively develops. Soot particles increase in mass and volume, their internal structure transforms from amorphous to graphite-like. Note that graphitization of the internal structure of soot particles is limited, when limit is reached the structure and properties stop active change, although the particles can still increase in size. Such soot particles are called mature. Fig. 3 presents examples of young and mature soot particles, and their internal structure.

The selected flames are equivalent to previously studied during past studies [5,7,6]. Table 2 presents basic results of these studies, where D — average size of particles, d — average interlayer spacing, $E(m, 1064)$ — function of refraction index at wavelength 1064 nm, E_g — optical band gap and T_{sub} — sublimation temperature. Both flames are characterized by direct correlation of properties with average size of particles. With rise of size of particles the interlayer spacing decreases from 0.43 to 0.35 nm, parameter $E(m, 1064)$ increases characterizing absorption of soot, and optical band gap decreases. But for the ethylene soot these processes occur at rise of particles size from 14.8 to 23 nm, but for the acetylene soot in range of particle size from 11.5 to 17.7 nm. This is especially clearly seen if we compare the sample of ethylene soot taken at a HAB 20 mm and the sample from acetylene flame at HAB 15 mm. They have close parameters of d, $E(m, 1064)$ and E_g, although the particle size differs by 33%. T_{sub} demonstrates evolution that differs from other parameters. For acetylene soot it rises from 2800 to 4050 K, for ethylene — from 4100 to 4500 K. From this we can conclude that T_{sub} depends only on size of particles and does not depend on fuel type [16].

It was decided to take sample of soot for study by Raman spectroscopy at HAB 5, 15 and 20 mm in flame acetylene–air and at HAB 5 and 20 mm in flame ethylene–air. HAB 5 and 20 mm correspond to young and mature soot. The soot particles at HAB 15 mm in flame acetylene–air are of interest as their parameters are close to those of the ethylene mature soot. The sampling was carried out on quartz plates of size $20 \times 10 \times 1$ mm. These plates using the pneumatic cylinder by pulse method were introduced horizontally into the flame center for 2 s (Fig. 1). Then beyond the flame they were cooled for 10 s in ambient air. This operation was repeated 50–100 times for the mature soot to accumulate sufficient amount of material for Raman spectroscopy.

1.3. Raman spectroscopy

Raman spectra of soot samples were measured in „InVia Reflex“ spectrometer („Reinshow“). For spectra excitation Nd: was used: YAG-laser with wavelength 532 nm. Power of radiation incident on the sample was 5.3 μW to exclude its structure damage. During measurements the laser beam was focused via a long-focus lens x50 into a circular area with diameter $\sim 2\,\mu$m. During measurement of Raman spectrum a diffraction grating with resolution 1800 gr/mm, measurement range from 100 to 3600 cm^{-1} was used. At each point, signal accumulation was carried out for 250 s. The device was calibrated as per silicon reference. In total 3 to 6 points were arbitrary selected on each sample to check the material homogeneity. Further these spectra were averaged to obtain statistically significant Raman spectrum.

Table 2. Properties of soot particles studied in papers [5,7,16]

	D, nm [5]	d, nm [5]	$E(m, 1064)$ [5]	E_g eV [7]	T_{sub}, K [16]	HAB, mm
C_2H_4	14.8	0.434	0.29	0.12 ± 0.05	4100 ± 164	10
	20	0.378	0.33	0.092 ± 0.05	4400 ± 177	13
	23	0.34	0.43	0.017 ± 0.05	4500 ± 180	20
C_2H_2	11.5	0.43	0.19	0.68 ± 0.05	2800 ± 112	5
	13.5	0.417	0.26	0.104 ± 0.05	2860 ± 114	10
	15.5	0.365	0.415	0.03 ± 0.05	3800 ± 152	15
	17.7	0.358	0.54	0.01 ± 0.05	4050 ± 160	20

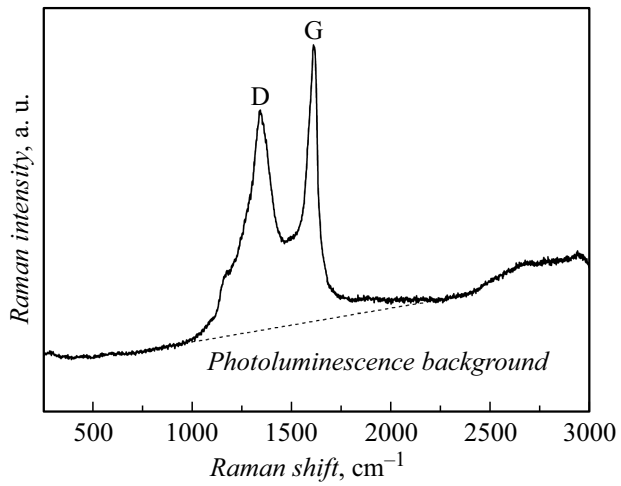

Figure 4. Averaged Raman spectrum of soot sample obtained in flame acetylene–air at HAB 5 mm. Dashed line shows background of photoluminescence.

2. Analysis of Raman spectra

Typical Raman spectrum of soot sample is presented in Fig. 4. We can note two basic features, namely peaks D and G which generally dominate in Raman spectrum of any disorder carbon materials [9]. The feature of Raman spectroscopy to provide chemical/structural information about carbon materials is that presence of defects in graphene layers of atoms with sp^2-hybridization allows to activate the Raman mode D („Defect“) at $\sim 1350\,\text{cm}^{-1}$, forbidden in ideal hexagonal lattice of graphene [20]. The edge effect in small graphene layers are one of the main sources of this peak. Peak G („Graphite“) at $\sim 1600\,\text{cm}^{-1}$ determined by each atom of carbon sp^2, on the contrary, is generally insensitive to defects and shows only small changes in the width and position of the maximum depending on different carbon structures [8]. Fig. 4 shows that Raman spectrum in addition to peaks D and G has continuous vertical component increasing with rise of Raman shift and determined by the presence of additional photoluminescence background.

It is well known that ratio of intensity of peaks D and G, $I(\text{D})/I(\text{G})$, can be expressed as function of size of graphene layers L_f comprising structure of soot particles [20]. Initially in graphite an inverse relationship between $I(\text{D})/I(\text{G})$ and L_f [20] was observed, but this relationship is true for materials with characteristic size L_f over 3 nm. When it comes to materials with graphene layer sizes below 3 nm, it stops working. Reason of this is that with decrease in L_f the number of aromatic rings decreases in single graphene domain which are responsible for peak D activation. As result, the intensity $I(\text{D})$ and ratio $I(\text{D})/I(\text{G})$ for the given materials show directly proportional dependence on L_f. Paper [8] shows that this dependence has quadratic view $I(\text{D})/I(\text{G}) \propto L_f^2$. Empirical expression for this dependence was given in paper [9] and has the following view:

$$L_f^2[nm^2] = 5.4 \cdot 10^{-2} \cdot (E_L)^4[eV^4] \cdot I(D)/I(G), \qquad (1)$$

where E_L — energy of incident photon.

In present paper the soot particles are discussed, which are highly disordered/amorphous carbon materials with graphene plane sizes below 2 nm [4,5]. So, in accordance with the results of papers [14,15] for Raman spectra interpretation formula (1) can be used. The peaks $I(\text{D})$ and $I(\text{G})$ from Raman spectra are determined using function of base line correction based on algorithm airPLS [21] (Fig. 5).

Typical Raman spectra of hydrated soot samples with excitation in visible range of spectrum comprise increase in background of photoluminescence with rise of Raman shift. This is associated with saturation by hydrogen of the nonradiative recombination centres, where they create intermediate levels in electron structure, intensifying radiative recombination and suppressing nonradiative one [22]. At content of H atoms over ~ 40–45% the background of photoluminescence generally does not exceed Raman signal.

Analysis of background photoluminescence in Raman spectrum can provide additional information on chemical composition of soot particles. Kaziragi et al. [23] derived an empirical equation that can be used to determine the content of hydrogen atoms in sample structure based on the measured ratio between the intensities of background of photoluminescence of Raman spectrum (m) and intensity of band $I(\text{G})$ (Fig. 5):

$$\text{H}[\%] = 21.7 + 16.6 \cdot \log_{10}\{m/I(G)\}, \qquad (2)$$

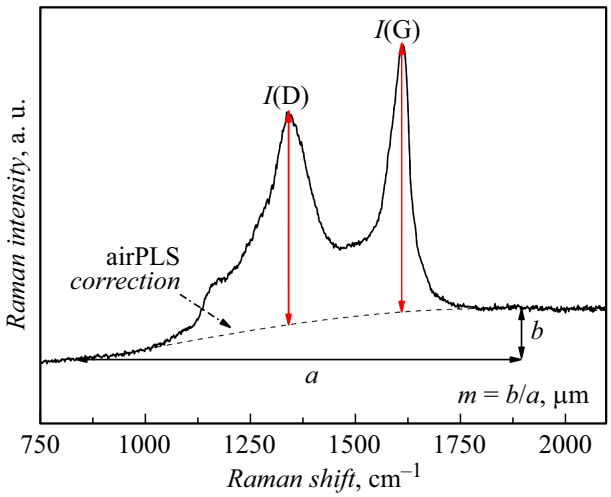

Figure 5. Interpretation of Raman spectrum of soot sampled in a flame acetylene–air at HAB 5 mm and determination of intensity peaks I(D), I(G) and background of photoluminescence m.

where H [at.%] — percent of hydrogen atoms used to calculate ratio H/C.

Note that in paper [23], where formula (2) was derived, the films of hydrated carbon, not soot particles were studied. As both materials are classified as carbon forms, where atoms have both sp^2-, and sp^3-hybridization, the authors consider it justified to use the formula (2) to obtain information on hydrogen content in structure of soot particles [15].

3. Results

Fig. 6 presented Raman spectra of soot particles obtained in flame. All spectra were normalized as per peak G. Images in left correspond to HAB 5 and 20 mm of flame ethylene–air. Images in right — to HAB 5, 15 and 20 mm of flame acetylene–air. As it was expected, all spectra contain clearly visible peaks D ($\sim 1350\,\text{cm}^{-}1$) and G ($\sim 1600\,\text{cm}^{-1}$) natural for carbon materials. Note that for both modes the following tendencies are observed, they are associated with flame height increasing:

1) intensity increasing of peak D relative to peak G which confirms growth of graphene layers in structure of soot particles;

2) decrease in background of photoluminescence associated with hydrogen content in soot particles.

At that spectra of acetylene soot at HAB 15 and 20 mm visually are similar, which can say that the active process of transformation of internal structure of particles in flame acetylene–air stop at HAB 15 mm. Besides, in spectra we can see presence of small additional peak in area of $\sim 1200\,\text{cm}^{-1}$. According to paper [13] this vibrational mode is activated by sp^2–sp^3-bonds or by tension of atoms C–C and C=C in aliphatic structures, but in present paper this is not analyzed.

In measured Raman spectra of soot the values of I(D)/I(G) were obtained. In flame ethylene–air they were 0.64 and 0.81 for young and mature soot particles, respectively. Use of equation (1) gives values of size of graphene layers $L_f = 1.01$ nm for HAB 5 mm and $L_f = 1.14$ nm for HAB 20 mm. Similarly the results were obtained for acetylene flame for HAB 5 mm — $I(\text{D})/I(\text{G}) = 0.8$, $L_f = 1.13$ nm; for HAB 15 mm — $I(\text{D})/I(\text{G}) = 0.99$, $L_f = 1.26$ nm, for HAB 20 mm — $I(\text{D})/I(\text{G}) = 1.02$, $L_f = 1.28$ nm. In Fig. 7 these values L_f are compared with average size of graphene layers obtained using TEM method [5], as well as with the results of study [14], where Raman method studied similar flame ethylene–air ([C]/[O] = 0.72). We can see that for soot particles synthesized in flame acetylene–air good matching is observed between values L_f obtained by TEM method (empty circles) and by Raman spectroscopy method (filled

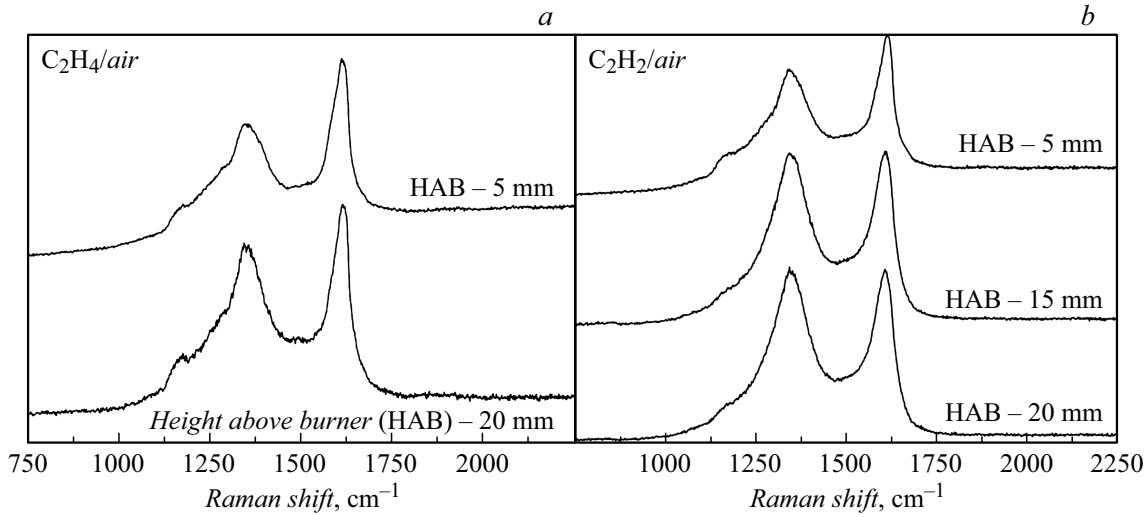

Figure 6. Raman spectra of soot particles taken at different HAB ethylene–air (a) and acetylene–air (b).

circles). For ethylene soot values of L_f, determined from Raman spectrum (filled squares), lie somewhat lower then results of electron microscopy (empty squares), by difference value does not exceed $\sim 18\%$, which can be assumed acceptable when two fundamentally different methods are used. Size of graphene layers 1–1.3 nm approximately corresponds to PAH molecule circumcoronene ($C_{54}H_{18}$) [25]. This is interesting observation which is in good agreement with the results of Wang's paper [25], where process of soot particles inception is discussed in detail, and where it is shown that PAH molecules only upon reaching the circumcoronene size can form dimers with sufficiently strong bonds to survive in flame conditions. For this the equilibrium constants of dimerization reaction K_p were compared for following PAH: coronene ($C_{24}H_{12}$), ovalene ($C_{32}H_{14}$) and circumcoronene ($C_{54}H_{18}$) with critical value K_p, necessary to keep dimer in conditions of soot flame at atmospheric pressure. It was shown that from three discussed PAHs only in circumcoronene the equilibrium dimerization constant is above the critical value in the temperature range 1600–1900 K natural for sooting flames, including studied in present paper (Fig. 2).

The important result of these measurements is significant increase in size of graphene layers with flame height increasing. It is well known that with HAB increasing not only structure changes, but also size of primary soot particles (see [4,26]). So, we can say that as the soot particles are formed with increase in HAB, increase in size of graphene planes in their structure occurs additionally to increase in total size of particles. On other hand data of measurement results made by TEM method in flames of different fuels in paper [5] did not identify changes of value of graphene layers upon growth of soot particles. In other words, according to TEM data soot particles, regardless of their size and growth stage, consisted of approximately the same structural elements. Actually, in Fig. 7, where empty symbols designate part of results from paper [5], we clearly view absence of systematic change in size of graphene layers obtained by TEM method, at different HAB, which corresponds to approximate constant value L_f, equal to 1.25 ± 0.1 nm (Fig. 7 — shaded area). But results of Raman spectroscopy obtained in present paper, and in paper [14] specify the presence of growth of graphene planes both for ethylene, and for acetylene soot upon increase in flame HAB. Considering the entire array of experimental data obtained in present paper and in studies [4,5,14] we can expect that size of graphene planes actually increases during growth of soot particles, but this size reaches limit value at the intermediate stage of particles formation, although particles themselves continue increasing in size and volume. In other words, at early stage of soot particles growth the graphene layers also grow but upon reaching the definite size of particles (~ 10 nm) the graphene layers reach maximum length (1.25 ± 0.1 nm [5]) and further growth of particles continues due to other mechanisms (coalescence, condensation, etc.).

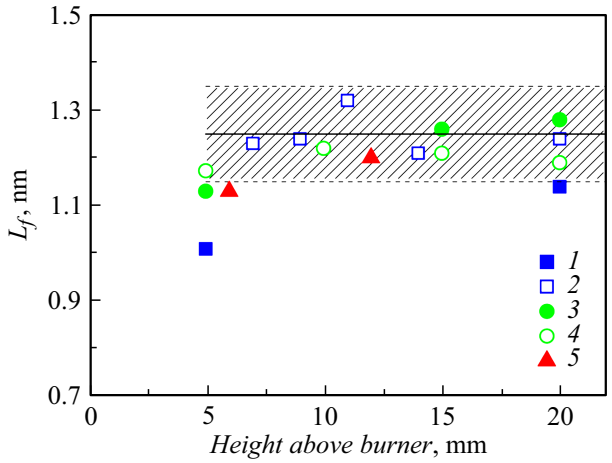

Figure 7. average length of graphene layers of soot particles depending on flame height above burner. Obtained results: *1* — by Raman method in flame ethylene–air, *2* — by TEM method in flame ethylene–air [5], *3* — by Raman method in flame acetylene–air, *4* — by TEM method in flame acetylene–air [5], *5* — by Raman method in flame ethylene–air ([C]/[O] = 0.72) [14]. Shaded area shows average size of graphene layers 1.25 ± 0.1 nm from paper [5].

Based on intensity measurements of background of photoluminescence in Raman spectra of soot in flame ethylene–air at HAB 5 and 20 mm the values of $m/I(\mathrm{G}) = 2.11 \pm 0.05\,\mu$m and $m/I(\mathrm{G}) = 0.58 \pm 0.05\,\mu$m were obtained, which using equation (2) ensures determination of the average percentage content of hydrogen atoms in soot particles $\mathrm{H} = 27.1 \pm 0.3\%$ and $\mathrm{H} = 17.8 \pm 0.8\%$ respectively. Such measurements were performed to study structure of the soot particles formed in flame acetylene–air at HAB 5, 15 and 20 mm. For HAB 5 mm the values $m/I(\mathrm{G}) = 1.3 \pm 0.05\,\mu$m and $\mathrm{H} = 23.6 \pm 0.4\%$ were obtained. For HAB 15 and 20 mm results are identical — $m/I(\mathrm{G}) = 0.23 \pm 0.05\,\mu$m and $\mathrm{H} = 11 \pm 1.8\%$. For both types of fuel upon flame height increasing there is decrease in percentage content of H atoms during growth of soot particles. At that for acetylene–air flame opposite to mode ethylene–air lower H content is natural for both young and mature soot particles.

H atoms in structure of soot particles is contained in form of organic carbon [14]. Presence of organic carbon inclusions has strong effect on structure and, as a result, on properties of soot particles (optical, thermophysical properties, tendency to oxidation, etc.). Fig. 8, *a* based on the obtained results shows how ratio H/C decreases during growth of soot particles with increase in HAB. As in Fig. 7, here for comparison the results of paper [14] are added, where by Raman method values $m/I(\mathrm{G})$ were determined for the similar flame ethylene–air ([C]/[O] = 0.72). From Fig. 7 and 8, *a* it is evident that zone of soot particles growth in paper [14] in conditions of ethylene flame was narrower than in present paper. But values of H/C of ethylene soot particles which both in present paper, and

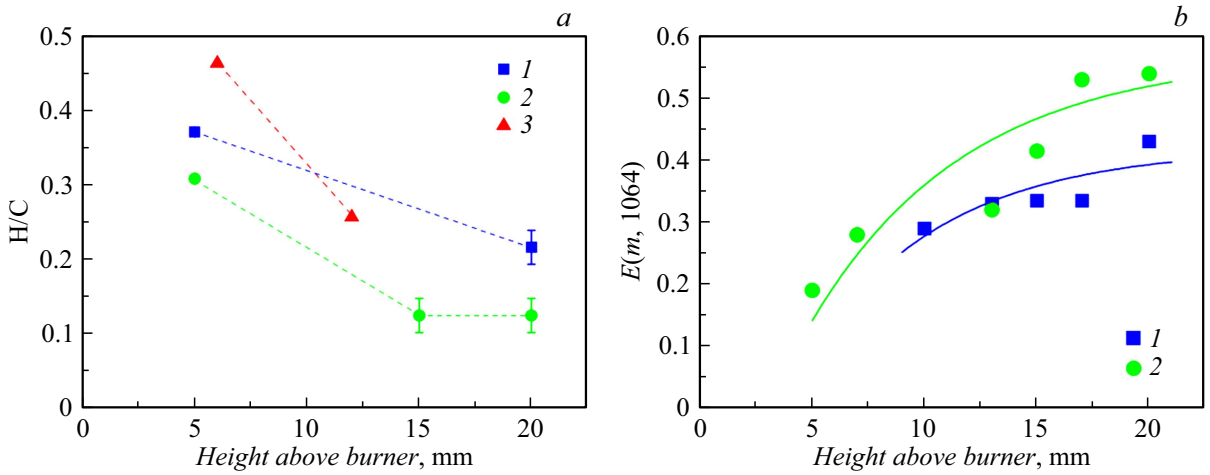

Figure 8. Change in properties of soot particles depending on HAB: *a* — ratio H/C, *b* — $E(m, 1064)$ from paper [5], where *1* — flame ethylene–air, *2* — flame acetylene–air, *3* — flame ethylene–air ([C]/[O] = 0.72) [14].

in paper [14] are identified as mature, have close value (0.21 and 0.26, respectively). At that the acetylene soot has lower H/C than ethylene soot in entire stage of soot particles growth from young and mature. Difference in values of H/C of flames from different fuels reaches maximum in range of HAB 15–20 mm, and is ~ 50%. Such a significant difference in the internal structure of the particles leads to difference in their optical properties. For comparison Fig. 8, *b* shows dependence of function of refraction index at wavelength 1064 nm $E(m, 1064)$ of soot particles on HAB obtained in paper [5] by method of laser-induced incandescence (LII) at flame parameters completely equivalent to the parameters used in the present paper (Table 1). In Fig. 8, *b* values $E(m, 1064)$ of acetylene soot exceed values $E(m, 1064)$ of ethylene soot in all HAB, where there was possibility to register LII signals. As $E(m, 1064)$ is directly linked with absorption coefficient for particles in the Rayleigh limit, we can conclude that soot particles from flame acetylene–air has better absorption than soot particles from flame ethylene–air, which qualitatively correlate with decrease in hydrogen content in particles composition.

As follows from Fig. 2, the temperature profiles differ in the flames studied. To HAB 7 mm temperature in both flames is equal to ~ 1750 K. With further HAB increasing the temperature in flame ethylene–air demonstrates quicker decreasing than in flame acetylene–air. Temperature difference in this section is ~ 100–150 K. In paper [27] difference in structure was studied of soot particles formed in flame of premixed gases methane–air at temperatures 1650 and 1770 K. It was demonstrated that the variation of structure of soot particles forming in a premixed flame depends more on the fuel characteristics than on the flame temperature [27,28]. If we compare the soot particles, studied at HAB 5 mm in both flame modes at equal temperatures, then we can conclude that in present paper studies of structure of soot particles synthesized in flame of different hydrocarbons at appropriate different temperature showed stronger correlation with fuel type than with flame temperature.

Paper [5] showed that reason of change in optical properties of soot particles during their growth is process of their graphitization: decrease in average interlayer and increase in volume of BSU regions in structure of soot particles, which is completely confirmed by data of Raman spectroscopy on size increase of graphene layers in structure of particles (Fig. 7). More over, results of Raman spectroscopy say that ratio H/C shall be also considered as parameter affecting the structure and properties of soot particles during their growth. It is expected that presence of H and degree of its decreasing during growth of particles directly depend on fuel type used for synthesis. The kinetic analysis of the differences in the pathways of soot particles formation from acetylene and ethylene requires separate study and is beyond the scope of this paper. But according to general accepted mechanism of soot formation HACA (hydrogen-abstraction-acetylene-addition) [29], acetylene is main „brick“ in process of soot particles growth [18]. It is expected that due to acetylene combustion mainly aromatic compounds are formed, they directly participate in process of soot particles growth. During ethylene combustion additionally to aromatic compounds the aliphatic structures are formed. Such compounds include acyclic hydrocarbons with groups CH_3 and CH_2 which contain large amount of hydrogen, and which can be in structure of soot particles in form of inclusions on edges of graphene layers. They slow down growth of graphene layers, decreasing intensity of oscillating mode D in Raman spectra, and increase relative fraction of H in structure of particles affecting the increase in photoluminescence signal. Indirect confirmation of this can be found in the work [30], where content of aliphatic structures in soot particles synthesized in flame ethylene and methane was compared. It was shown that during combustion of methane as fuel less prone to soot formation, the content of aliphatic structures in soot particles was

higher than in ethylene soot. As ratio H/C in methane is by two times higher than in ethylene, the content of hydrogen in methane soot also was higher, and its absorption was lower. Acetylene as fuel for synthesis of soot particles in paper [30] was not considered, so our assumption requires experimental confirmation.

Conclusion

Method of Raman spectroscopy studied soot particles synthesized in premixed flames ethylene–air and acetylene–air. Comparison of parameters of particles synthesized under given conditions is performed for the first time. Sampling was performed at HAB corresponding to intermediate and final stages of particles formation.

It was observed that graphene layers — base elements of structure of soot particles — grow in size with HAB increasing. For flame ethylene–air size of graphene layers L_f increases from 1.01 to 1.14 nm, for flame acetylene–air — from 1.13 to 1.28 nm. The obtained results supplement data obtained previously by TEM method indicating the process of size increasing of graphene layers L_f at initial stages of soot particles growth. Size of graphene layers 1–1.3 nm corresponds to polyaromatic molecule of circumcoronene with number of carbon atoms 54.

It was shown that content of hydrogen in soot particles decreased with HAB increasing. For flame ethylene–air H content decreases from $27.1 \pm 0.3\%$ to $17.8 \pm 0.8\%$; for flame acetylene–air — from $23.6 \pm 0.4\%$ to $11 \pm 1.8\%$. The dehydrogenation process reflects change in the internal structure of soot particles during their growth and is one of the processes characterizing the graphitization of particles along with increase in the volume of BSU regions inside the soot particles and decrease in the average interlayer spacing.

The acetylene soot demonstrates more graphitize structure than ethylene soot which is expressed in large values L_f and lower content of H during growth of soot particles. It is expected that reason of this is lower content of aliphatic structures formed during acetylene combustion as compared to the ethylene. Results obtained under present study can be applied in climatic models, to clarify the contribution of soot particles to atmospheric heating, and to improve the methods of monitoring the aerosols containing soot particles.

Acknowledgments

The authors thank A.A. Averin (A.N. Frumkin Institute of Physical Chemistry and Electrochemistry of the Russian Academy of Sciences) for assistance in measuring the samples.

Funding

This study was supported financially by the Ministry of Science and Higher Education of the Russian Federation, State Assignment № 075-00270-24-00.

Conflict of interest

The authors declare that they have no conflict of interest.

References

[1] E.V. Gurentsov, A.V. Eremin, R.N. Kolotushkin. Atmos. Oceanic Opt, **35** (6), 645 (2022). DOI: 10.1134/S102485602206015X

[2] T.C. Bond, S.J. Doherty, D.W. Fahey, P.M. Forster, T. Berntsen, B.J. DeAngelo, M.G. Flanner, S. Ghan, B. Kärcher, D. Koch, S. Kinne, Y. Kondo, P.K. Quinn, M.C. Sarofim, M.G. Schultz, M. Schulz, C. Venkataraman, H. Zhang, S. Zhang, N. Bellouin, S.K. Guttikunda, P.K. Hopke, M.Z. Jacobson, J.W. Kaiser, Z. Klimont, U. Lohmann, J.P. Schwarz, D. Shindell, T. Storelvmo, S.G. Warren, C.S. Zender. J. Geophys. Res. Atmos., **118**, 5380 (2013). DOI: 10.1002/jgrd.50171

[3] G. De Falco, Ch. Colarusso, M. Terlizzi, A. Popolo, M. Pecoraro, M. Commodo, P. Minutolo, M. Sirignano, A. D'Anna, R.P. Aquino, A. Pinto, A. Molino, R. Sorrentino. Front. Immunol., **8**, 1415 (2017). DOI: 10.3389/fimmu.2017.01415

[4] B. Apicella, P. Pre, M. Alfe, A. Ciajolo, V. Gargiulo, C. Russo, A. Tregrossi, D. Deldique, J.N. Rouzaud. Proc. Combust. Inst. **35**, 1895 (2015). DOI: 10.1016/j.proci.2014.06.121

[5] E.V. Gurentsov, A.V. Drakon, A.V. Eremin, R.N. Kolotushkin, E.Yu. Mikheyeva. High Temperature, **60** (3), 335 (2022). DOI: 10.1134/S0018151X22020055

[6] H.A. Michelsen, M.B. Colket, P.-E. Bengtsson, A.D. Anna, P. Desgroux, B.S. Haynes, J.H. Miller, G.J. Nathan, H. Pitsch, H. Wang. ACS Nano, **14** (10), 12470 (2022). DOI: 10.1021/acsnano.0c06226

[7] E.V. Gurentsov, A.V. Eremin, R.N. Kolotushkin, E.S. Khodyko. Bull. Lebedev Phys. Inst., **49** (12), 422 (2022). DOI: 10.3103/S1068335622120028

[8] A.C. Ferrari, J. Robertson. Philos. Trans. R. Soc. A, **362**, 2477 (2004). DOI: 10.1098/rsta.2004.1452

[9] A.C. Ferrari, D.M. Basko. Nat. Nanotechnol., **8**, 235 (2013). DOI: 10.1038/nnano.2013.46

[10] M. Lapuerta, F. Oliva, J.R. Agudelo, J.P. Stitt. Combust. Sci. Technol., **183** (11), 1203 (2011). DOI: 10.1080/00102202.2011.587484

[11] H. Ge, Z. Ye, R. He. J. Environ. Sci. (Beijing, China), **79**, 74 (2019). DOI: 10.1016/j.jes.2018.11.001

[12] E. Villa-Aleman, J.R. Darvin, M.H. Nielsen, T.M. Willey. J. Raman Spectrosc., **53**, 1571 (2022). DOI: 10.1002/jrs.6401

[13] B. Dippel, H. Jander, J. Heintzenberg. Phys. Chem. Chem. Phys., **1**, 4707 (1999). DOI: 10.1039/A904529E

[14] S. Bocchicchio, M. Commodo, L.A. Sgro, M. Chiari, A. D'Anna, P. Minutolo. Fuel, **310**, 122306 (2022). DOI: 10.1016/j.fuel.2021.122308

[15] C. Russo, A. Ciajolo. Combust. Flame, **162**, 2431 (2015). DOI: j.combustflame.2015.02.011

[16] E.V. Gurentsov, A.V. Drakon, A.V. Eremin, R.N. Kolotushkin, E.Yu. Mikheyeva. Tech. Phys., **92** (1), 53 (2022). DOI: 10.21883/TP.2022.01.52533.206-21

[17] B. Axelsson, R. Collin, P.-E. Bengtsson. Appl. Opt., **39**, 3683 (2000). DOI: 10.1364/AO.39.003683

[18] T.V. Komarova. *Poluchenie uglerodnykh materialov* (D.I. Mendeleev RKhTU, M., 2001) (in Russian)

[19] C.S. McEnally, Ü.Ö. Köylü, L.D. Pfefferle, D.E. Rosner. Combust. Flame, **109** (4), 701 (1997). DOI: 10.1016/S0010-2180(97)00054-0
[20] F. Tuinstra, J.L. Koenig. J. Chem. Phys., **53**, 1126 (1970). DOI: 10.1063/1.1674108
[21] Z.-M. Zhang, S. Chen, Y.-Z. Liang. Analyst, **135** (5), 1138 (2010). DOI: 10.1039/B922045C
[22] J. Robertson. Phys. Rev. B, **53**, 16302 (1996). DOI: 10.1103/PhysRevB.53.16302
[23] C. Casiraghi, F. Piazza, A.C. Ferrari, D. Grambole, J. Robertson. Diamond Relat. Mater., **14**, 1098 (2005). DOI: 10.1016/j.diamond.2004.10.030
[24] Y. Zou, X. Hou, H. Wei, J. Shao, Q. Jiang, L. Ren, J. Wu. Angew. Chem., **62** (19), e2023010 (2023). DOI: 10.1002/anie.202301041
[25] H. Wang. Proc. Combust. Inst., **33** (1), 41 (2011). DOI: 10.1016/j.proci.2010.09.009
[26] A.V. Drakon, A.V. Eremin, E.V. Gurentsov, E.Yu. Mikheyeva, R.N. Kolotushkin Appl. Phys. B: Lasers Opt., **127** (6), 81 (2021). DOI: 10.1007/s00340-020-07426-3
[27] M. Alfe, B. Apicella, J.-N. Rouzaund, A. Tregrossi, A. Ciajolo. Combust. Flame, **157** (10), 1959 (2010). DOI: 10.1016/j.combustflame.2010.02.007
[28] M. Alfe, B. Apicella, R. Barbella, J.N. Rouzaud, A. Tregrossi, A. Ciajolo. Proc. Combust. Inst., **32** (1), 697 (2009). DOI: 10.1016/j.proci.2008.06.193
[29] H. Wang, M. Frenklach. Combust. Flame, **110**, 173 (1997). DOI: 10.1016/S0010-2180(97)00068-0
[30] C. Russo, A. Tregrossi, A. Ciajolo. Proc. Combust. Inst., **35**, 1803 (2015). DOI: 10.1016/j.proci.2014.05.024

Translated by I.Mazurov